ASN NEURO RESEARCH ARTICLE

ASN NEURO 1(2):art:e00006.doi:10.1042/AN20090015

Memory deficits in APP23/*Abca1*$^{+/-}$ mice correlate with the level of Aβ oligomers

Iliya Lefterov*[1], Nicholas F Fitz*, Andrea Cronican*, Preslav Lefterov*, Matthias Staufenbiel[†] and Radosveta Koldamova*[1]
*Department of Environmental and Occupational Health, University of Pittsburgh, Pittsburgh, PA 15219, U.S.A.
[†]Department of Nervous System, Novartis Institutes of Biomedical Research, CH-4002 Basel, Switzerland

Cite this article as: Lefterov I, Fitz NF, Cronican A, Lefterov P, Staufenbiel M and Koldamova R (2009) Memory deficits in APP23/*Abca1*$^{+/-}$ mice correlate with the level of Aβ oligomers. ASN NEURO 1(2):art:e00006.doi:10.1042/AN20090015

ABSTRACT

ABCA1, a member of the ATP-binding cassette family of transporters, lipidates ApoE (apolipoprotein A) and is essential for the generation of HDL (high-density lipoprotein)-like particles in the CNS (central nervous system). Lack of Abca1 increases amyloid deposition in several AD (Alzheimer's disease) mouse models. We hypothesized that deletion of only one copy of *Abca1* in APP23 (where APP is amyloid precursor protein) AD model mice will aggravate memory deficits in these mice. Using the Morris Water Maze, we demonstrate that 2-year-old *Abca1* heterozygous APP23 mice (referred to as APP23/het) have impaired learning during acquisition, and impaired memory retention during the probe trial when compared with age-matched wild-type mice (referred to as APP23/wt). As in our previous studies, the levels of ApoE in APP23/het mice were decreased, but the differences in the levels of Aβ and thioflavin-S-positive plaques between both groups were insignificant. Importantly, dot blot analysis demonstrated that APP23/het mice have a significantly higher level of soluble A11-positive Aβ (amyloid β protein) oligomers compared with APP23/wt which correlated negatively with cognitive performance. To confirm this finding, we performed immunohistochemistry with the A11 antibody, which revealed a significant increase of A11-positive oligomer structures in the CA1 region of hippocampi of APP23/het. This characteristic region-specific pattern of A11 staining was age-dependent and was missing in younger APP23 mice lacking *Abca1*. In contrast, the levels of Aβ*56, as well as other low-molecular-mass Aβ oligomers, were unchanged among the groups. Overall, the results of the present study demonstrate that in aged APP23 mice memory deficits depend on Abca1 and are likely to be mediated by the amount of Aβ oligomers deposited in the hippocampus.

Key words: ABCA1, *Abca1*-knockout mouse, Alzheimer's disease, amyloid β protein, apolipoprotein E (ApoE), APP transgenic mouse.

INTRODUCTION

AD (Alzheimer's disease) is senile dementia characterized by extracellular amyloid plaques and intracellular neurofibrillary tangles. Amyloid plaques comprising fibrillar Aβ (amyloid β protein) are thought to be central to AD pathogenesis. Previously, three different groups have reported that global deletion of *Abca1* (ATP-binding cassette transporter 1), in AD model mice [APP (amyloid precursor protein) transgenic mice] increased the level of Aβ plaques in the brain; however, cognitive function was not examined (Hirsch-Reinshagen et al., 2005; Koldamova et al., 2005a; Wahrle et al., 2005). ABCA1 exports cholesterol and phospholipids from cells on to lipid-poor apolipoproteins (ApoA-I, ApoE and others) and forms nascent HDL (high-density lipoprotein) particles. The transcriptional activation of *ABCA1* and *APOE* (in both humans and mice) is controlled by nuclear LXRs (liver X receptors) α and β (LXRα/β) (Tontonoz and Mangelsdorf, 2003), and our previous studies have demonstrated that the effect of LXRs on soluble Aβ is mediated through ABCA1 (Tontonoz and Mangelsdorf, 2003; Koldamova et al., 2005b; Koldamova and Lefterov, 2007). Mutations in human *ABCA1* cause severe HDL deficiencies, the most prominent of which is Tangier disease, characterized by the virtual absence of ApoA-I and HDL, accumulation of cholesterol in cells and prevalent atherosclerosis (Oram and Heinecke, 2005). ABCA1 also has an important role in the CNS (central nervous system); it is responsible for the lipidation of ApoE and the formation of HDL-like lipoproteins, which transport cholesterol in the brain. Studies have shown that the lack of Abca1 in mice

[1] Correspondence may be addressed to either of these authors (email iliyal@pitt.edu or radak@pitt.edu).
Abbreviations: Aβ, amyloid β protein; ABCA1, ATP-binding cassette transporter 1; AD, Alzheimer's disease; ApoE, apolipoprotein E; APP, amyloid precursor protein; CNS, central nervous system; DAPI, 4′,6-diamidino-2-phenylindole; GFAP, glial fibrillary acidic protein; HDL, high-density lipoprotein; LXR, liver X receptor; MWM, Morris Water Maze; PBST, PBS containing 0.2% Triton X-100; Thio-S, thioflavin S; X-34, 1,4-bis(3-carboxy-4-hydroxyphenylethenyl)-benzene.

greatly reduces the levels of ApoE, probably caused by an increased degradation of abnormally lipidated ApoE (Hirsch-Reinshagen et al., 2004; Wahrle et al., 2004). It has been reported that the elevation in amyloid plaque load in APP/*Abca1*^{ko} mice is accompianed by a dramatic decrease in soluble ApoE, with no change in insoluble ApoE (Hirsch-Reinshagen et al., 2005; Koldamova et al., 2005a; Wahrle et al., 2005). In contrast, the overexpression of Abca1 in PDAPP [PDGF (platelet-derived growth factor) APP] mice resulted in less amyloid plaques than in PDAPP mice expressing a normal level of Abca1 (Wahrle et al., 2008).

In the present paper we report the effects of Abca1 on spatial learning and memory retention in APP transgenic mice (the APP23 line), by comparing cognitive performance of 22–24-month-old APP23 mice with one or two copies of the *Abca1* gene using the MWM (Morris Water Maze) paradigm. We chose to examine *Abca1* heterozygous mice instead of *Abca1* knockout mice because the global deletion of *Abca1* (in *Abca1* knockout mice) or two non-functional copies of *ABCA1* (as in Tangier disease) should be considered an extreme example. Reduced ABCA1 transport function due to genetic variants, rather than complete loss of the transporter, is common in the human population and is often accompanied by distinct clinical phenotypes (Oram and Heinecke, 2005). Previous studies have shown that APP23 mice display memory deficits demonstrated by impaired learning during acquisition in the MWM, although the performance during the probe trial was not impaired in all studies (Kelly et al., 2003; Van Dam et al., 2003, 2005). Our results demonstrate that the lack of only one copy of *Abca1* impaired spatial learning in APP23 mice. Surprisingly, the memory deficits in APP23/*Abca1* heterozygous mice did not correlate with amyloid load, but to the level of soluble Aβ oligomers in their brain.

MATERIALS AND METHODS

Transgenic mice

All animal experiments were approved by the University of Pittsburgh Institutional Animal Care and Use Committee. Two well-characterized model mouse lines were used to set up breeding pairs and to generate experimental groups. APP23 transgenic mice express the human familial AD mutant APP751 with Swedish double mutations at positions 670/671 (APPK670N, M671L) (Sturchler-Pierrat et al., 1997). The expression of human APPsw is driven by the murine Thy-1 promoter and is restricted to neurons. *Abca1*$^{+/-}$ heterozygous mice, originally generated by McNeish et al. (2000) at Pfizer, were obtained from Jackson Laboratories, line DBA/1-*Abca1*^{tm1Jdm}/J. *Abca1*$^{+/-}$ mice were crossed to APP23 mice (C57BL/6 background) to generate the APP23/*Abca1*$^{+/-}$ (APP23/het) progeny. The progeny were identified by PCR and APP23/het mice were bred to *Abca1*$^{+/-}$ littermates to yield APP23/*Abca1*$^{+/-}$ (APP23/het) and APP23/*Abca1*$^{+/+}$ (APP23/wt) bigenic littermate mice (Koldamova et al., 2005a). Thus all APP23/het and APP23/wt mice used in the present study are hemizygous APP23. APP23/het developed similarly to APP23/wt and no gross anatomical abnormalities were observed until 24 months of age. For the purpose of the present study we used mice of two ages with the following genotypes: APP23/het (ten females and three males), APP23/wt (13 females and four males), both groups at 22–24 months of age, and APP23/wt or APP23/Abca1$^{-/-}$ (APP23/ko) mice at 13 months of age. In addition, for behavioural tests we used 22–24-month-old wild-type (wt/wt) mice and mice with one copy of a functional *Abca1* gene (*Abca1*$^{+/-}$ referred to as wt/het) as APP non-transgenic littermate controls.

MWM

A modified version of the MWM was used to assess spatial navigation learning and memory retention. The water maze studies were conducted in the Rodent Behavior Analysis Core of the University of Pittsburgh Health Sciences Department. In a circular pool of water (diameter 100 cm, height 30 cm, temperature 25$\pm$1°C) we measured the ability of mice to form a representation of the spatial relationship between a safe, but invisible (submerged 1 cm below the water level), platform (10 cm in diameter), and visual cues surrounding the pool of water. The platform was located in the centre of one of the four quadrants of the pool. Several extra maze cues were distributed across the walls surrounding the pool. Animals received two habituation trials (one per day) during which the animals were handled for several minutes by the experimenter and allowed to explore the pool of water without the platform present. Beginning the next day, they received four daily hidden platform training (acquisition) trials with 10–12 min inter-trial intervals for four consecutive days. Animals were allowed 60 s to locate the platform and 40 s to rest on it. Mice that failed to find the platform were placed on the platform by the experimenter and allowed to rest there for 40 s. At 24 h following the last acquisition trial, a single 60 s probe trial was administered to assess spatial memory retention. For the probe trial, animals were returned to the maze as during training, but with no platform present. Performance was recorded with an automated tracking system (SMART; San Diego Instruments) during all training and probe trials. During the acquisition trials, latency to reach the platform and path length (distance swum to the platform) were subsequently used to analyse and compare the performance between different groups of mice. The relative time spent in each of the four quadrants and the number of crossings of the former platform location were recorded and analysed during the probe trials.

Animal tissue processing

Mice were anaesthetized with Avertin (250 mg/kg of body weight, intraperitoneal injection; Sigma) and perfused

transcardially with 25 ml of 0.1 M PBS (pH 7.4). Brains were rapidly removed, divided into hemispheres, and the olfactory bulbs and cerebellum were removed. One hemisphere was snap-frozen on dry ice and the other was drop fixed in 4% phosphate-buffered paraformaldehyde at 4°C for 48 h before being stored in 30% sucrose.

Histology and immunohistochemistry

All procedures were as reported previously (Koldamova et al., 2005a) with the following modifications. Histoprep (Fisher Scientific)-embedded hemibrains were cut in the coronal plane at 30 μm sections on a cryostat and stored in a glycol-based cryoprotectant at −20°C until immunostained. Sections were selected 700 μm apart, starting from a randomly chosen section approx. 150 μm caudal to the first appearance of the CA3 and dentate gyrus. Sections were mounted on Superfrost Plus slides (Fisher Scientific) and outlined with a delimiting pen (DakoCytomation). After sections were washed in PBST (PBS containing 0.2% Triton X-100), non-specific binding was blocked by incubating the sections for 1 h in PBST with 3% normal goat serum (Sigma). Sections were incubated either overnight at 4°C or for 3 h at room temperature (22°C) with one of the following antibodies: polyclonal rabbit anti-GFAP (glial fibrillary acidic protein) antibody (1:1000; DakoCytomation) or polyclonal rabbit anti-oligomer antibody (A11; 1:600; Invitrogen). The anti-GFAP antibody recognizes the principal intermediate filament of mature astrocytes and A11 recognizes a peptide backbone epitope common to amyloid oligomers, but not found in native proteins, amyloidogenic monomer or mature amyloid fibrils. Sections were washed in PBST and incubated at room temperature for 1 h in the corresponding secondary antibody: Alexa Fluor® 546-conjugated goat anti-mouse IgG (1:1000; Molecular Probes) or Texas Red-conjugated goat anti-rabbit IgG (1:1000, Molecular Probes). The specificity of the staining was confirmed by the lack of signal when applying the same protocol on brain sections from non-transgenic wild-type mice.

For Thio-S (thioflavine S) staining, mounted sections were processed essentially as previously described (Koldamova et al., 2005a). Sections mounted on Superfrost Plus slides were post-fixed in 10% formalin for 10 min, washed in PBS, incubated in 0.25% potassium permanganate for 10 min, bleached in a solution containing 2% potassium metabisulfate and 1% oxalic acid until they appeared white, and finally stained for 10 min in 0.015% Thio-S in 50% ethanol. After washing in 50% ethanol and water, the slides were dried before being coverslipped with Fluoromount-G (Southern Biotech).

X-34 [1,4-bis(3-carboxy-4-hydroxyphenylethenyl)-benzene] is a highly fluorescent derivative of Congo Red that can be used to detect senile plaques and was provided by Dr W. Klunk (Department of Psychiatry, University of Pittsburgh, Pittsburgh, PA, U.S.A.). X-34 staining was performed on mounted sections as described previously (Ikonomovic et al., 2006). Briefly, sections mounted on Superfrost Plus slides were post-fixed in 10% formalin for 10 min, washed in PBS for 5 min and stained with X-34 (100 μM) for 10 min. Following the staining, sections were washed in distilled water, incubated in 0.2% NaOH in 80% unbuffered ethanol, washed again, and soaked for 10 min in distilled water. Slides were dried and coverslipped with Fluoromount-G/DAPI (4′,6-diamidino-2-phenylindole) nuclear stain.

Microscopic examination was carried out using a Nikon Eclipse 80i microscope and images were captured by a Nikon DS Qi1MC camera. For quantitative analysis, immunostaining in the neocortex and hippocampus was defined as the percentage area covered by immunoreactivity, Thio-S or X-34 positivity. The percentage of immunoreactivity and positivity was determined by examining the entire area of interest for each section using Nikon Elements v3.0 software. Confocal microscopy was performed on an Olympus Fluoview 1000 inverted confocal microscope.

Aβ ELISA and Western blot analysis

Aβ ELISA and Western blot analysis were performed essentially as described in Koldamova et al. (2005a). The frozen hemibrains (only cortices and hippocampi) were homogenized in THB [tissue homogenization buffer; 250 mM sucrose, 20 mM Tris base, 1 mM EDTA, 1 mM EGTA (pH 7.3), 1 ml per 150 mg of tissue) and protease inhibitors {10 μg/ml leupeptin, 10 μg/ml aprotinin and 10 μg/ml AEBSF [4-(2-aminoethyl)benzenesulfonyl fluoride]}. Protein extracts were prepared by a 1:1 dilution of the initial homogenate with 2 × RIPA {10 mM Tris/HCl (pH 7.3), 1 mM $MgCl_2$, 0.25% SDS and 1% Triton X-100 in the presence of protease inhibitors [10 μg/ml leupeptin, 10 μg/ml aprotinin and 10 μg/ml 4-(2-aminoethyl)benzenesulfonyl hydrochloride]} buffer in the presence of protease inhibitors and Western blot analysis for Abca1, ApoE and APPfl were performed as previously described (Koldamova et al., 2005a). To examine Aβ oligomers on Western blotting, the proteins were resolved on 4–12% Bis-Tris gels (Invitrogen) and probed with the 6E10 antibody. Extraction of soluble and insoluble Aβ was carried out as described in Koldamova et al. (2005a). An ELISA for Aβ was performed using 6E10 as the capture antibody, and anti-Aβ40 (G2-10 mAb) and anti-Aβ42 (G2-13 mAb) monoclonal antibodies conjugated to horseradish peroxidase (Genetics Company) were used as the detection antibodies. The final values of Aβ were based on Aβ-(1–40) and Aβ-(1–42) peptide standards (Bachem Biosciences) and normalized amounts of Aβ were expressed as pmol/mg of protein.

Brain soluble Aβ oligomer analysis

The level of soluble Aβ oligomers was measured by dot blot assay as described previously (Kayed et al., 2003, 2007) with slight modification. Briefly, soluble amyloid peptide was extracted in RIPA buffer containing protease inhibitors (see above). After centrifugation at 100 000 ***g*** for 1 h at 4°C, the supernatant was analysed. Samples (1 μg) of total protein were spotted on to nitrocellulose membrane and probed with the A11 antibody (1:1000), specific for oligomeric forms of Aβ. The

immunoreactive signals were visualized using an ECL (enhanced chemiluminescence) detection kit (GE Healthcare) and were quantified densitometrically (Image Quant). The exact same samples were spotted on to additional dot blots and probed with 6E10 and Bradford reagent for normalization.

Statistical analysis

All results are reported as means ± S.E.M. Statistical significance for ELISA, Western blotting and dot blotting data was determined using a two-tailed Student's *t* test. Significant differences between mean scores during acquisition trial blocks in the MWM were assessed with two-way repeated measures ANOVA (General Linear Model/RM-ANOVA) with Tukey's post-hoc analysis for multiple comparisons using genotype and trial block number as sources of variation. A two-tailed Student's *t* test was used to evaluate the difference between the number of crossings through the platform location during the probe trial. Comparisons of percentage immunoreactivity between ages and genotypes were performed using one-way ANOVA with Tukey's post-hoc analysis. To determine a correlation between variables the data were analysed by scatter plot and by Pearson correlation analysis. Significance was defined as $P \leq 0.05$. All statistical analyses were performed in GraphPad Prism, version 4.0 or SPSS, version 16, release 200.

RESULTS

Abca1 deficiency exacerbates cognitive performance in APP23 mice

To assess Abca1 effects on cognitive performance we used the MWM paradigm and tested spatial learning and memory retention in 22–24-month-old APP23/het and APP23/wt mice. Age-matched wt/wt and wt/het mice were used as APP non-transgenic controls.

During the acquisition phase, as illustrated by the learning curves in Figure 1, all groups improved their performance with increased training. RM-ANOVA analysis revealed a significant main effect of the trial block on both dependent variables: distance swum to the platform or path length ($P<0.001$) and escape latency ($P<0.001$). Between subjects, the factor genotype had a significant effect only on the path length ($P<0.001$), but not on the escape latency. One-way ANOVA demonstrated a significant difference between the groups ($P<0.001$) for path and escape latency ($P<0.05$) on the last two trial days. APP23/wt learned significantly slower than non-transgenic wt/wt mice (wt/wt compared with APP23/wt: day 2 and 3, path length, $P<0.05$ and $P<0.01$; day 3, escape latency, $P<0.05$), although their performance ultimately reached control levels on the last day of the training phase (Figures 1A and 1B). In contrast, APP23/het never learned this task as efficiently as non-transgenic wt/het mice. Most importantly, as visible from learning curves in Figures 1(A) and 1(B), APP23/wt mice displayed better spatial acquisition compared with APP23/het animals demonstrated by the differences in both path length (Figure 1A; 235 ± 27 cm compared with 407 ± 45 cm, $P<0.01$) and escape latency (Figure 1B; 19.88 ± 1.9 s compared with 28.98 ± 2.69 s; $P<0.01$) on the last day of the training. No significant differences were identified in the learning curves between wt/het and wt/wt non-transgenic mice.

At 24 h after the last training session, mice were tested in a probe trial during which search patterns were monitored in the absence of a platform. As visible from Figure 1(C), APP23/wt, as well as the non-transgenic controls, had normal spatial memory retention. In contrast, APP23/het had significantly fewer numbers of crossings over the original target location

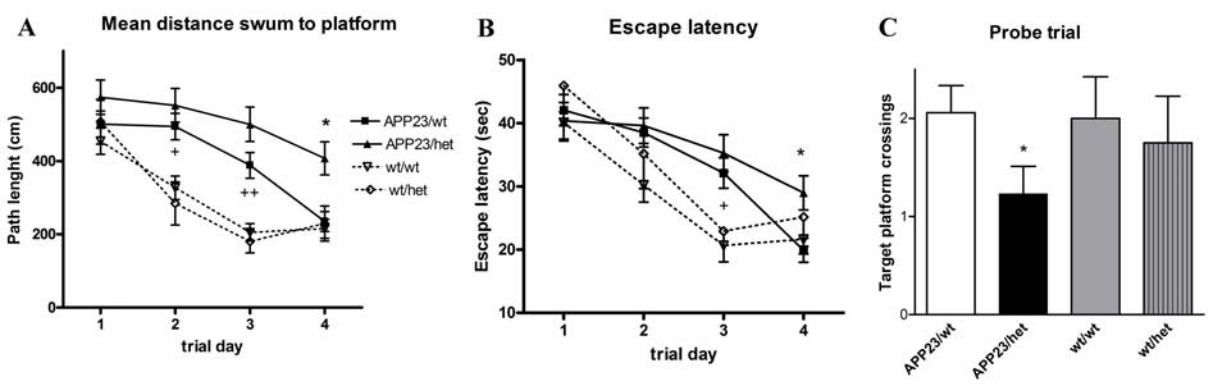

Figure 1 **Abca1 deficiency exacerbates cognitive deterioration in APP23 mice: MWM tests**

(**A**) Mean distance swum to the platform (path lengths) represents the average distance to find the platform. $P<0.001$ for trial days 2, 3 and 4 (as measured by one-way ANOVA analyses). (**B**) Escape latency scores represent average acquisition time taken to find the platform, per trial block. $P<0.05$ for trial days 3 and 4 (as measured by one-way ANOVA). In (**A**) and (**B**), *$P<0.05$ APP23/het compared with APP23/wt; +$P<0.05$ and ++$P<0.01$ APP23/wt compared with wt/wt (as measured using a Tukey's post-hoc test). (**C**) Probe trial. Platform crossings are calculated as the number of crosses over the exact location of the hidden platform. *$P<0.05$ APP23/het compared with APP23/wt (as measured by two-tailed Student's *t* test analysis). All values represent means ± S.E.M. All mice tested were between 22 and 24 months of age. APP23/wt $n=17$, APP23/het $n=13$, wt/wt $n=13$ and wt/het $n=4$ mice per group.

than APP23/wt mice, suggesting worsened memory retention (Figure 1C; 2.1 compared with 1.2, $P<0.05$). The difference in performance at any test point could not be attributed to lower swimming velocity of the APP23/het mice, as two-way RM-ANOVA revealed no significant difference among the groups ($P>0.1$ in all comparisons; results not shown). Our conclusion is that *Abca1* deficiency exacerbates spatial memory in APP23 mice, exemplified by worsened cognitive performance during both the acquisition and retention phases of MWM paradigm.

Cognitive decline in APP23/het mice does not correlate with the level of insoluble amyloid in their brain

Previous work from our group and others have demonstrated that the lack of Abca1 significantly affects both brain ApoE protein levels and its degradation, and increases amyloid deposition in APP transgenic mice (Hirsch-Reinshagen et al., 2005; Koldamova et al., 2005a; Wahrle et al., 2005). Similarly to our previous studies (Koldamova et al., 2005a) we found that the level of soluble ApoE in the brains of APP23/wt mice with two intact copies of *Abca1* was significantly higher than in APP23/het animals (Figure 2A, $P<0.05$). In terms of amyloid phenotype, the level of soluble Aβ40 (RIPA extraction) was decreased and that of Aβ42 was unchanged (Figure 2B). Corresponding to the decreased soluble Aβ40, APP23/het had significantly more Aβ40 in the insoluble brain fraction (formic acid extraction), compared with APP23/wt, whereas the levels of insoluble Aβ42 did not differ (Figure 2C). To determine the relationship between the level of insoluble Aβ40 and Aβ42, and the performance in the MWM, we performed a correlation analysis. Scatter plots shown in Figures 2(D) and 2(E) demonstrate that there was no correlation between the number of crossings over the target platform and Aβ40 ($P=0.51$) or Aβ42 ($P=0.82$).

To determine how the amyloid pathology corresponds to the memory deficits in mice subjected to behavioural testing, the amount of Aβ deposited into plaques was also examined

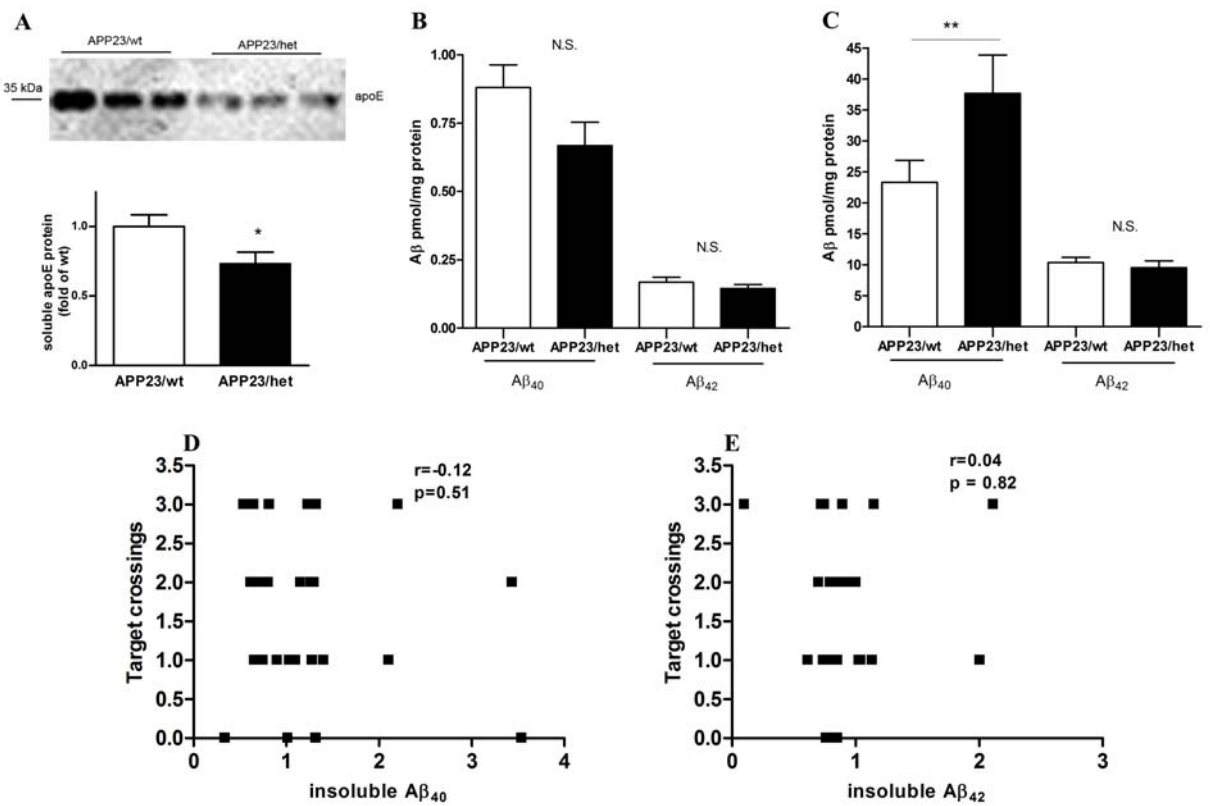

Figure 2 **The level of insoluble Aβ does not correlate with the cognitive deficits in APP23/het and APP23/wt mice**
(**A**) Soluble ApoE was extracted from cortices and hippocampi using DEA and the level was determined by Western blot analysis. (**B** and **C**) Aβ was sequentially extracted from cortices and hippocampi of 24-month-old APP23/wt and APP23/het mice first using RIPA (soluble fraction) followed by formic acid (insoluble fraction) and Aβ40 and Aβ42 was measured by ELISA. Assessment of (**B**) soluble Aβ and (**C**) insoluble Aβ. *$P<0.05$ and **$P< 0.01$ (as measured using a two-tailed Student's *t* test). (**D** and **E**) Relationship between probe trial performance in MWM and levels of insoluble Aβ40 (**D**) and Aβ42 (**E**) in 24-month-old APP23/wt and APP23/het. Levels of insoluble Aβ in individual mice were normalized to the average levels in APP23/wt mice. Note that there was no correlation between insoluble Aβ40 and Aβ42 and the numbers of target crossings during the probe trial. $n=13–16$ per group.

using immunohistochemistry. Brain sections were stained with Thio-S for detection of compact parenchymal Aβ deposits and cerebral amyloid angiopathy (Figures 3A and 3B). Parametric ANOVA revealed no significant effect of *Abca1* genotype. Similarly, there was no significant difference in the percentage of Thio-S-positive staining in the hippocampus (P=0.78). Reactive gliosis is a common feature associated with various factors for AD, which may play a role in the progression of AD. Senile plaques are surrounded by high levels of reactive astrocytes producing pro-inflammatory cytokines and reactive oxygen species, which exacerbate the amyloid pathology and cognitive decline observed in APP transgenic mice (Town et al., 2008; Zhou et al., 2008). To determine the level of astrogliosis, brain sections from APP23/wt and APP23/het mice were immunostained for GFAP. Although high levels of GFAP-labelled astrocytes surrounded Thio-S-positive plaques (Figure 3C), there was no difference in GFAP immunostaining when comparing 24-month-old APP23/wt and APP23/het mice. In addition, we measured mRNA expression of a number of pro-inflammatory cytokines [TNF-α (tumour necrosis factor-α), IL-6 (interleukin-6), IL-1β and iNOS (inducible nitric oxide synthase)] using our routine protocol for real-time quantitative PCR (Lefterov et al., 2007), but did not find a difference between wild-type (APP23/wt) and heterozygous (APP23/het) mice (results not shown).

Cognitive decline in APP23/het mice correlates with the level of soluble Aβ oligomers in their brains

Synaptic dysfunction caused by the accumulation of soluble Aβ oligomers (Kayed et al., 2003; Lesne et al., 2006; Shankar et al., 2008) could be a possible explanation for the memory impairment seen in APP23/het mice. We first examined the level of Aβ dodecameric (56 kDa) Aβ42 assemblies (Aβ*56), recently suggested as a reason for memory deficits in APP-expressing Tg2576 mice (Lesne et al., 2006). To determine whether Aβ*56 changes with aging we performed Western blot analysis of RIPA-extracted brain proteins (cortex and hippocampus) with the 6E10 antibody. The results demonstrated that there was an age-dependent increase in the level of the 56 kDa 12-mer Aβ oligomer in APP23 mice making it a potential marker for memory function in this AD mouse

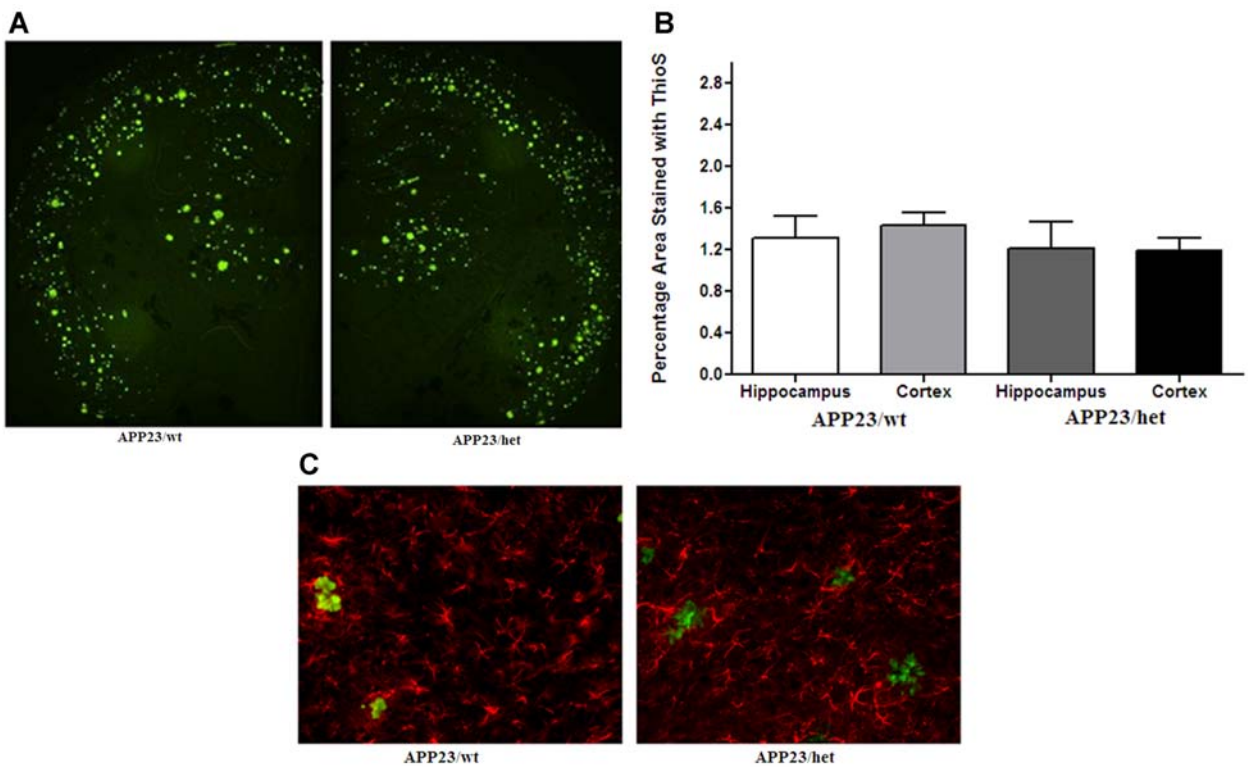

Figure 3 **Histological analysis of Thio-S-positive amyloid deposits in 24-month-old APP23 mice**
(**A**) Brain sections from APP23/wt and APP23/het mice were stained with Thio-S to visualize fibrillar amyloid plaques. The images represent the approximate average levels of Thio-S-positive plaques (20×). (**B**) Graphical representation of the area of the cortex and hippocampus covered by Thio-S-positive deposits. (**C**) Brain sections were immunostained with an anti-GFAP antibody to show reactive astrogliosis and was co-stained with Thio-S for amyloid plaques (200×). n=12 for APP23/wt and n=11 for APP23/het.

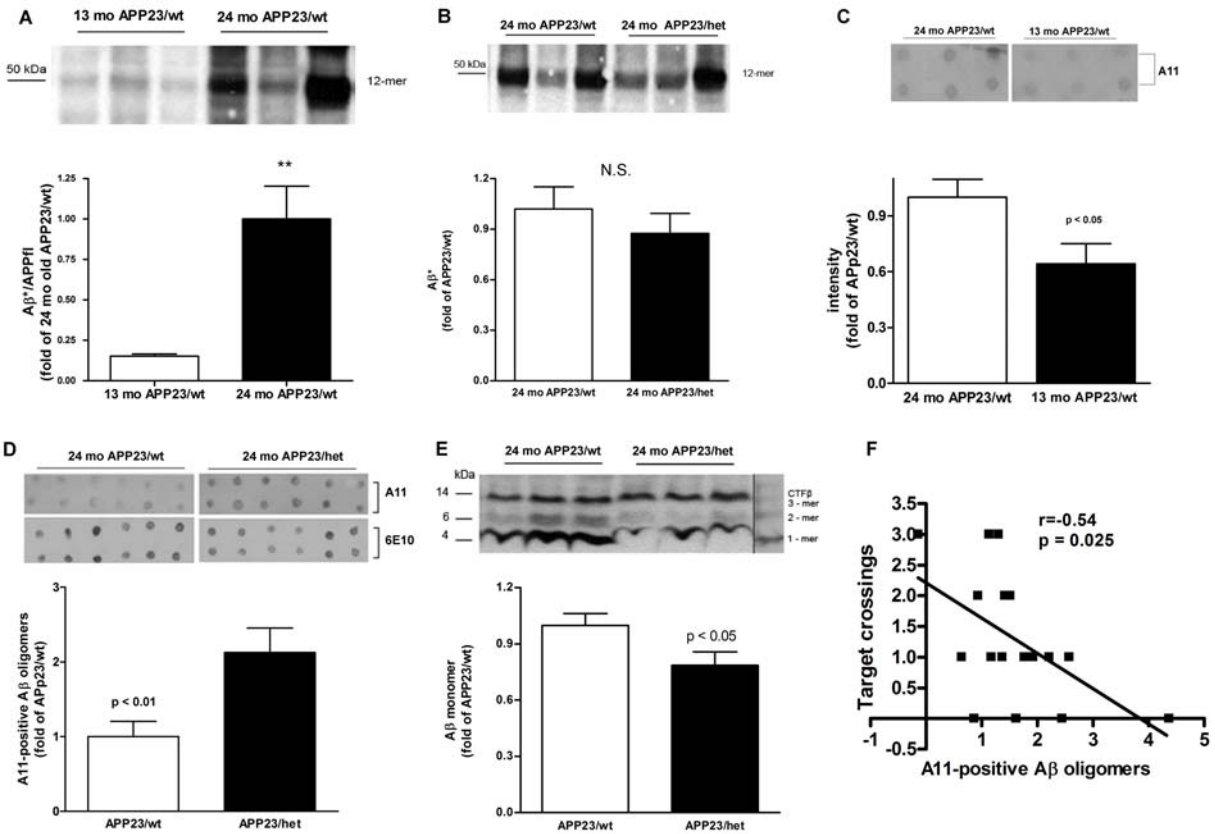

Figure 4 **The level of soluble Aβ oligomers is increased in APP23/het mice**

Aβ was extracted with RIPA from cortices and hippocampi of 13-month-old APP23/wt, and 24-month-old APP23/wt and APP23/het mice and Western and dot blot analyses were performed using 6E10 and A11 anti-oligomeric antibodies respectively. (**A** and **B**) Comparison of 56 kDa Aβ* in 13- and 24-month-old APP23/wt mice (**A**, $n=6$ per group), and 24-month-old APP23/wt and APP23/het (**B**, $n=13$ per group) was performed using Western blot analysis with the 6E10 antibody (representative Western blots are shown above the histograms). Note the variability in Aβ*56 intensity in older mice. All Western blots were repeated three times. (**C**) Dot blot assessment of Aβ oligomers using the A11 antibody comparing samples from 13-month-old APP23/wt and 24-month-old APP23/wt mice ($n=8$). A representative dot blot is shown above the histogram. (**D**) Dot blot assessment of Aβ oligomers using the A11 antibody comparing samples from 24-month-old APP23/wt and APP23/het mice. The upper panel shows representative dot blots using the A11 antibody; the lower panel shows a representative dot blot using the same samples processed with the 6E10 antibody ($n=8$). (**E**) Western blot analysis of the Aβ monomer in APP23/wt and APP23/het mice using the 6E10 antibody ($n=13$). Values in (**A**–**E**) represent means $\pm$ S.E.M. (**F**) Relationship between probe trial performance in MWM and levels of soluble A11-positive oligomers in 24-month-old mice. Scatter plot and Pearson correlation analysis were used to determine the relationship between the level of A11-positive oligomers and performance at the probe trial. Note that there is a negative (Pearson $r=-0.54$), statistically significant, correlation ($P=0.025$) between the level of A11 oligomers and the number of crossings of the exact area of the target platform in APP23/wt and APP23/het ($n=8$–9 per group). For (**A**–**F**), the levels of 6E10- and A11-positive oligomers in individual mice were normalized to the average levels in 24-month-old APP23/wt mice.

model. Figure 4(A) shows that, compared with 13-month-old APP23/wt mice, there was a 6-fold increase of Aβ*56 in 24-month-old APP23/wt mice. However, there was no difference in Aβ*56 levels in 24-month-old APP23/wt and APP23/het mice (Figure 4B) and no correlation with the performance in the MWM. It has to be noted that there was variability in the level of Aβ*56 in the older group of mice illustrated by the representative blot on Figure 4(B). Additional examination of other Aβ low-molecular-mass oligomer species detected at molecular masses theoretically corresponding to trimeric (14 kDa), hexameric (27 kDa) and nonameric (40 kDa) Aβ42 assemblies also did not show a significant difference between APP23/wt and APP23/het groups (results not shown).

Next, we used the A11 anti-oligomeric antibody, which was shown to detect higher-molecular-mass Aβ oligomers on dot and Western blotting (Kayed et al., 2003, 2007). Figure 4(C) shows that, in APP23/wt mice at 13 months and 24 months, there is an age-dependent increase of Aβ oligomers recognized by A11 ($P<0.05$). Similar dot blot analysis demonstrated that A11 immunoreactivity was increased more than 2-fold in 24-month-old APP23/het mice as compared with 24-month-old APP23/wt mice (Figure 4D; $P<0.01$; upper panels of the inset are representative dot blots with the A11 antibody). Previously it has been demonstrated that, on a dot blot, 6E10 antibody detects Aβ monomers and Aβ fibrils, but not prefibrillar oligomer Aβ (Kayed et al., 2007;

Necula et al., 2007). Therefore we also compared the samples from 24-month-old APP23/het and APP23/wt mice performing dot blotting with 6E10 antibody. As shown in Figure 4(D) there is no difference in 6E10 immunoreactivity on dot blots from samples of 24-month-old APP23/het and APP23/wt mice (Figure 4D; lower panels of the inset are representative dot blots with 6E10). This confirms the results from ELISA and Thio-S staining, that there is no difference in the fibrillar amyloid among APP23/wt and APP23/het mice (see also Figures 2C, 3A and 3B). To prove that the amount of protein loaded on to the dots was equal, they were pre-stained with Bradford reagent (results not shown). We also found that, in accordance with the increased level of Aβ oligomers in APP23/het mice, there was a statistically significant decrease in the level of Aβ monomers in these mice when compared with APP23/wt (Figure 4E; $P<0.05$). To determine the relationship between the level of A11-positive oligomers and performance in the MWM, the data were analysed by correlation analysis. The scatter plot shown in Figure 4(F) demonstrates that there was a negative ($r=-0.54$) and statistically significant ($P=0.025$) correlation between the level of A11 oligomers and the number of crossings over the target platform in wild-type and heterozygous APP23 mice during the probe trial.

Increased A11 immunoreactivity in the CA1 region of the hippocampus of 24-month-old APP23/het compared with APP23/wt mice

To confirm the preceding finding using a different method, we performed immunohistochemistry with the A11 antibody on sections from cortices and hippocampi. We compared the following groups of mice: 13-month-old APP23/wt and APP23/ko, and 24-month-old APP23/wt and APP23/het. We specifically chose APP23/ko mice instead of APP23/het in the younger group because our previous results did not show any significant difference between Aβ load in APP23/wt and APP23/het at 13 months of age (Koldamova et al., 2005a). We examined different regions of the hippocampus: CA1, CA2 and septum. As shown in Figure 5(A), when compared with other groups, 24-month-old APP23/het demonstrated a striking increase of A11 immunoreactivity in the CA1 region of the hippocampus. The quantification and analysis of A11

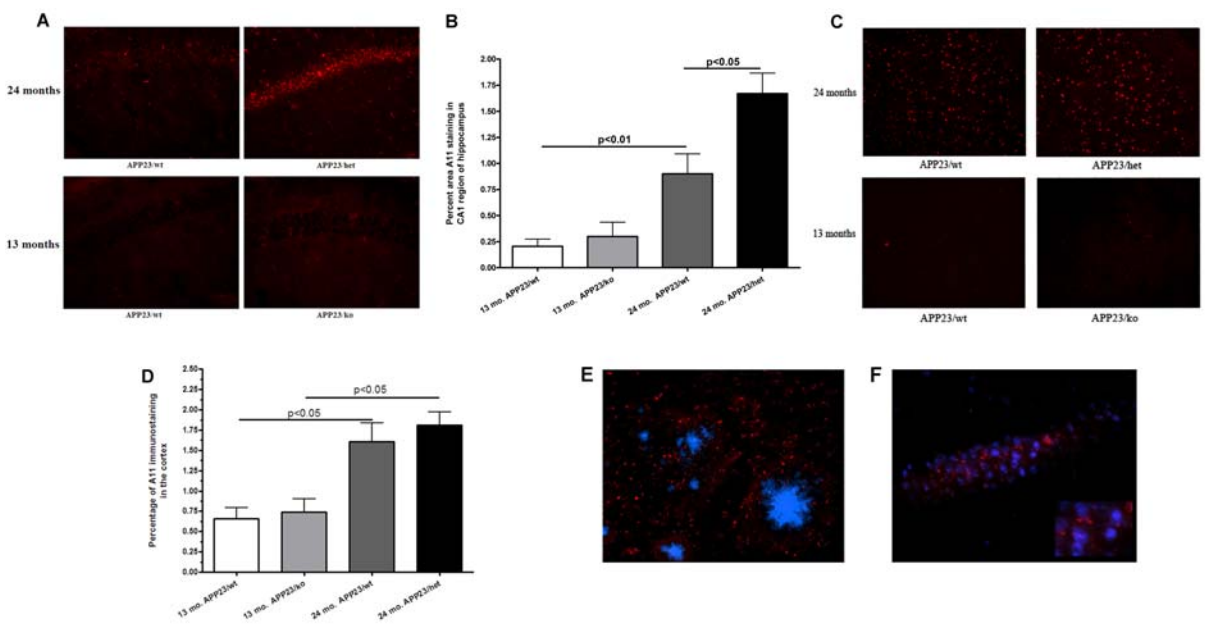

Figure 5 **A11 immunostaining in the hippocampus of 13- and 24-month-old mice**

(**A**) The CA1 region of hippocampi from APP23 mice stained with the A11 antibody to visualize soluble oligomers. The images represent the approximate average levels of A11 immunostaining in both young and old mice (100 ×). (**B**) The histogram represents the percentage area of the hippocampi covered by A11-immunolabelled oligomers. $n=6$ mice per group. Statistics by one-way ANOVA and Tukey's multiple comparison post-hoc tests. Note a significant effect of age ($P<0.01$ when 13-month-old APP23/wt are compared with 24-month-old APP23/wt) and genotype ($P<0.05$ when 24-month-old APP23/wt are compared with 24-month-old APP23/het). (**C**) Representative images of A11 immunoreactivity in the cortex of 13- and 24-month-old APP23 mice. (**D**) Histogram representing the percentage area of the cortex covered by A11-immunolabelled oligomers. $n=6$ mice per group. Note a significant effect of age ($P<0.05$ when 13-month-old APP23/wt are compared with 24-month-old APP23/wt), but not of genotype (no statistical significance when 24-month-old APP23/wt are compared with 24-month-old APP23/het). (**E**) Brain section from APP23/wt co-stained with the A11 antibody and DAPI (1000 ×, confocal microscopy). A11 immunostaining is located outside the nucleus but mostly in the cell body layer of CA1. (**F**) Representative brain section from APP23/wt co-stained with the X-34 and A11 antibodies (400 ×). A11 immunostaining is located outside fibrillar amyloid plaques.

immunostaining by one-way ANOVA demonstrated that there was a substantial and statistically significant difference among the groups ($P<0.001$; Figure 5B). Post-hoc analysis showed that A11 immunoreactivity within the CA1 significantly increased with age (Figure 5B). For example, 24-month-old APP23/wt mice had 4-fold more A11 staining than 13-month-old APP23/wt (0.8100 ± 0.2078 and 0.2049 ± 0.06877 respectively, $P<0.01$). To determine the effect of the genotype we first compared younger APP23/wt and APP23/ko mice at 13 months of age. As shown in Figure 5(B), A11 immunostaining in 13-month-old APP/ko mice was slightly, but not significantly, increased compared with APP23/wt mice (0.2049 ± 0.06877 compared with 0.2991 ± 0.1370, $P>0.05$). However, significantly more A11 immunostaining was observed in the CA1 of 24-month-old APP23/het mice when compared with age-matched APP23/wt mice (1.669 ± 0.1963 compared with 0.8100 ± 0.2078, $P<0.001$). These results suggest that A11-positive oligomers in the CA1 region of the hippocampus in the examined mice depend on the *Abca1* genotype and their amount increases with aging.

In the cortex of 24-month-old APP23/wt and APP23/het mice there was no significant difference in A11 immunostaining (Figure 5C). Similarly, there was no significant difference in A11 immunostaining in the cortex of 13-month-old APP23/wt and APP23/ko mice (Figure 5C). However, there was significantly more A11 immunostaining in 24-month-old APP23/wt mice when compared with 13-month-old APP23/wt (Figures 5B and 5C; 1.53 compared with 0.73, $P<0.05$), suggesting an age-related increase in A11 immunostaining in the cortex.

To further determine the location of A11 immunostained oligomers, we performed co-staining of brain sections from 24-month-old APP23/wt mice to label nuclei and senile plaques. Brain sections co-stained with A11 and DAPI nuclear stain showed A11 immunostaining surrounding, but situated outside, the nucleus in both the cortex and hippocampus. Interestingly, within the hippocampus, A11-immunostained oligomers were located almost exclusively in the cell body layer of the CA1 region (Figures 5E and 5F). Brain sections co-stained with A11 antibody and X-34 showed A11 immunostaining located outside fibrillar plaque formations (Figure 5F).

DISCUSSION

In the present paper, we describe novel findings that memory deficits in 2-year-old APP23 mice depend on *Abca1* gene dosage and are likely to be mediated by the amount of Aβ oligomers deposited in the hippocampus. We used the MWM to assess spatial learning and memory retention in age-matched APP23/wt and APP23/het mice. When compared with APP23/wt mice, APP23/het mice demonstrated impaired learning during the acquisition phase, as well as impaired memory retention during the probe trial. Importantly, we found a significant difference in the level of soluble A11-positive Aβ oligomers which correlates negatively with the cognitive performance. Furthermore, there was an unexpected region-specific redistribution of Aβ oligomer structures, predominantly in the CA1 of APP23/het mice. Thus the results of the present study implicate *Abca1* deficiency in the development of behavioural deficits which are an important aspect of AD pathogenesis. Taken together, the results contribute to further understanding the significance of the Abca1–ApoE axis in AD model mice, suggesting a role in the development of cognitive impairments along with already proven effects of these proteins on amyloid deposition and clearance.

There are several possible explanations for the worse memory performance of APP23/het compared with APP23/wt mice in the MWM. First, the amount and possibly the distribution of oligomeric Aβ deposited in brain could be responsible, although the precise mechanism by which amyloid fibrils or soluble aggregates impair the cognition of APP transgenic mice remains to be elucidated. Notably, Aβ can exist as monomers, low-molecular-mass oligomers such as dimers, trimers, Aβ*56, larger globular oligomers (ADDL, amylospheroids, and globulomers), protofibrils, fibrils and amyloid plaques (Lambert et al., 1998; Hoshi et al., 2003; Kayed et al., 2003; Lesne et al., 2006; Chimon et al., 2007; Shankar et al., 2008). However, it is not clear which of these Aβ assemblies is causative for the memory decline observed in AD. Other evidence suggests that non-fibrillar assemblies of Aβ play a critical role in the pathogenesis of AD (Lambert et al., 1998; Hoshi et al., 2003; Kayed et al., 2003; Lesne et al., 2006; Chimon et al., 2007; Shankar et al., 2008). Studies from transgenic AD models, and organotypic and cell culture models have provided convincing support that soluble Aβ can be detrimental to many key neuronal activities. In the present study, we found that there was an age-dependent increase in the level of Aβ*56 oligomer in APP23 mice, suggesting that potentially it could be a marker for memory function in this model, as in other APP transgenic mice (Lesne et al., 2006; Billings et al., 2007). However, the level of Aβ*56 oligomer was unchanged in 24-month-old APP23/wt compared with APP23/het mice. In contrast, our results demonstrate that the increase of A11-positive Aβ oligomers depends not only on the age, but also on *Abca1* genotype. As demonstrated in Figure 4, in 24-month-old APP23/het mice the amount of A11-positive Aβ oligomers is increased 2-fold compared with age-matched APP23/wt mice, and this increase correlated negatively with their performance during the MWM probe trial. Furthermore, there was a corresponding increase of A11 immunoreactivity in the CA1 region in the hippocampus of those mice, which was strikingly different, compared with what was observed in APP23/wt mice. As in other AD models (Maezawa et al., 2008) we found A11 staining in the CA1 to be mostly intracellular. This pattern of staining with deposits comprising Aβ accumulations in neurons, observed only in

the CA1, but not in other regions, of the hippocampus, was recently reported in human *APOE4*, but not in human *APOE3*, targeted replacement (knock-in) mice. These characteristic intracellular Aβ42 aggregates, which were A11-positive and likely to be Aβ oligomeric structures, also corresponded to the memory deficits in those mice (Belinson et al., 2008). In addition, in brain sections from APP23 mice of all ages examined in the present study and regardless of the *Abca1* genotype, the extracellular staining with A11 antibody was spatially segregated from the plaques, similar to human AD brain (Kayed et al., 2003).

Insoluble Aβ, amyloid plaques and plaque-associated neuritic dystrophy have all been assigned a pathogenic role with abundant evidence linking the extent of learning and memory impairment as well as behavioural deficits to amyloid burden and the amount of insoluble Aβ in APP-expressing mice. However, in a difference from oligomeric Aβ we did not find a correlation between the increased levels of insoluble Aβ40 and performance in MWM. Furthermore, there was no statistically significant difference in the levels of insoluble Aβ and Thio-S-positive plaques between APP23/wt and APP23/het groups.

Based on previous studies and the results of the present study we propose that an increase of soluble oligomeric Aβ in specific brain areas, most prominently in the CA1 region of the hippocampus, rather than the elevated amount of insoluble Aβ40 itself, contributes to the cognitive deterioration of aged APP23/het animals. At this point we can only speculate about the reason why Aβ oligomers are increased in APP23/het mice. A potential reason may be the decreased total amount of ApoE, which was significantly lower in APP23/het compared with APP23/wt mice (Figure 2A). It has been demonstrated that in Tg-SwDI mice complete absence of ApoE increased the amount of soluble Aβ oligomers in brain parenchyma in spite of markedly decreasing depositions of insoluble Aβ and with no effect on total brain Aβ (Miao et al., 2005). Furthermore, binding of Aβ to normally lipidated ApoE and ApoA-I, which depends on functional and properly expressed *Abca1*, could decrease the formation of Aβ aggregates, such as fibrils, protofibrils or globular oligomers. For example, it was demonstrated that the ApoE effect on Aβ aggregation depends on its lipidation status, with lipid-rich ApoE being more effective in decreasing Aβ aggregation (LaDu et al., 1994, 1995; Maezawa et al., 2004). In addition, experiments with neuronal cell lines have shown that ApoA-I binding to Aβ decreases its aggregation and toxicity (Koldamova et al., 2001; Maezawa et al., 2004).

It is also possible that the difference in the performance of APP23/wt and APP23/het mice could be linked to brain lipoprotein metabolism and cholesterol transport within the brain and between neurons and glia. In a series of elegant studies, Pfrieger and colleagues showed that the ability of CNS neurons to form synapses is limited by the availability of cholesterol (Pfrieger and Barres, 1997; Mauch et al., 2001). CNS neurons synthesize enough cholesterol to survive and grow, but the formation of numerous mature synapses demands additional amounts that must be provided by glia. Synaptogenesis requires large amounts of cholesterol and therefore depends on its delivery via ApoE-containing lipoproteins (Pfrieger and Barres, 1997; Mauch et al., 2001). The present study indicates that, in the brain of APP23/het mice, there is less ApoE, which may lead to insufficient amounts of cholesterol being delivered to surrounding axons and therefore less efficient synaptogenesis. One possible consequence of the less efficient synaptogenesis is a behavioural deficit. Results from recently published studies with LXR ligands confirm such a possibility: it has been shown that application of synthetic LXR ligands (T0901317 and GW3965) improves memory deficits in Tg2576 mice (Riddell et al., 2007; Jiang et al., 2008). The main conclusion from these studies is that LXR-dependent mechanisms in the brain, most probably mediated through the established Abca1–ApoE axis, are responsible for the beneficial effect of the ligands. More importantly, these mechanisms could be amenable to pharmacological modulation if proper LXR ligands become available in the future.

In addition, the results of the present study suggest that heterozygous *Abca1* mice could be considered a valuable model when overexpressing human genes related to AD types of neurodegeneration, or with global disruption of genes involved in neurological disorders known for perturbed neuronal development or impaired synaptic plasticity. In terms of their impaired cholesterol metabolism, heterozygous *Abca1* mice show an intermediate phenotype between *Abca1*^{wt} and *Abca1*$^{-/-}$ (Koldamova et al., 2005a). The beneficial effect of *ABCA1*^{wt} homozygosity in humans is underscored by numerous studies demonstrating perturbed cholesterol and lipoprotein homoeostasis in individuals heterozygous for *ABCA1* mutant alleles. Therefore *Abca1* heterozygous mouse models (presumably ones that carry mutant, clinically significant alleles), rather than mice completely lacking *Abca1* should be considered more relevant to study the influence of perturbed brain cholesterol metabolism on molecular pathogenesis and progression of different neurodegenerative disorders.

Lastly, although previous studies have examined the effect of Abca1 on brain amyloid deposition and clearance in APP transgenic mice (Hirsch-Reinshagen et al., 2005; Koldamova et al., 2005a; Wahrle et al., 2005), to our knowledge our present study is the first investigation addressing the role of Abca1 on cognitive performance. Previous studies have demonstrated that global deletion of *Abca1* substantially increases amyloid deposition in the brain parenchyma and vasculature, possibly through facilitated Aβ aggregation. In addition, recent data suggest that properly lipidated brain ApoE and ApoA-I lipoproteins are necessary for Aβ degradation and clearance of amyloid deposits (Jiang et al., 2008; Wahrle et al., 2008). Such findings present evidence for the important regulatory function of Abca1 in brain cholesterol homoeostasis and AD pathology, and provide a rationale for behavioural studies, such as the present study, examining the role of Abca1 in AD model animals.

ACKNOWLEDGEMENTS

We thank Dr E. Thiels and the Rodent Behavior Core Facility at the University of Pittsburgh, School of Medicine for assistance with the MWM.

FUNDING

This work was supported by NIA (National Institute on Aging) [grant numbers AG027973, AG023304, AG028794, AG031956], and an Alzheimer's Association award.

REFERENCES

Belinson H, Lev D, Masliah E, Michaelson DM (2008) Activation of the amyloid cascade in apolipoprotein E4 transgenic mice induces lysosomal activation and neurodegeneration resulting in marked cognitive deficits. J Neurosci 28:4690–4701.

Billings LM, Green KN, McGaugh JL, LaFerla FM (2007) Learning decreases Aβ*56 and tau pathology and ameliorates behavioral decline in 3xTg-AD mice. J Neurosci 27:751–761.

Chimon S, Shaibat MA, Jones CR, Calero DC, Aizezi B, Ishii Y (2007) Evidence of fibril-like β-sheet structures in a neurotoxic amyloid intermediate of Alzheimer's β-amyloid. Nat Struct Mol Biol 14:1157–1164.

Hirsch-Reinshagen V, Zhou S, Burgess BL, Bernier L, McIsaac SA, Chan JY, Tansley GH, Cohn JS, Hayden MR, Wellington CL (2004) Deficiency of ABCA1 impairs apolipoprotein E metabolism in brain. J Biol Chem 279:41197–41207.

Hirsch-Reinshagen V, Maia LF, Burgess BL, Blain JF, Naus KE, McIsaac SA, Parkinson PF, Chan JY, Tansley GH, Hayden MR, Poirier J, Van NW, Wellington CL (2005) The absence of ABCA1 decreases soluble ApoE levels but does not diminish amyloid deposition in two murine models of Alzheimer disease. J Biol Chem 280:43243–43256.

Hoshi M, Sato M, Matsumoto S, Noguchi A, Yasutake K, Yoshida N, Sato K (2003) Spherical aggregates of β-amyloid (amylospheroid) show high neurotoxicity and activate tau protein kinase I/glycogen synthase kinase-3β. Proc Natl Acad Sci USA 100:6370–6375.

Ikonomovic MD, Abrahamson EE, Isanski BA, Debnath ML, Mathis CA, DeKosky ST, Klunk WE (2006) X-34 labeling of abnormal protein aggregates during the progression of Alzheimer's disease. Methods Enzymol 412:123–144.

Jiang Q, Lee CY, Mandrekar S, Wilkinson B, Cramer P, Zelcer N, Mann K, Lamb B, Willson TM, Collins JL, Richardson JC, Smith JD, Comery TA, Riddell D, Holtzman DM, Tontonoz P, Landreth GE (2008) ApoE promotes the proteolytic degradation of Aβ. Neuron 58:681–693.

Kayed R, Head E, Thompson JL, McIntire TM, Milton SC, Cotman CW, Glabe CG (2003) Common structure of soluble amyloid oligomers implies common mechanism of pathogenesis. Science 300:486–489.

Kayed R, Head E, Sarsoza F, Saing T, Cotman CW, Necula M, Margol L, Wu J, Breydo L, Thompson JL, Rasool S, Gurlo T, Butler P, Glabe CG (2007) Fibril specific, conformation dependent antibodies recognize a generic epitope common to amyloid fibrils and fibrillar oligomers that is absent in prefibrillar oligomers. Mol Neurodegener 2:18.

Kelly PH, Bondolfi L, Hunziker D, Schlecht HP, Carver K, Maguire E, Abramowski D, Wiederhold KH, Sturchler-Pierrat C, Jucker M, Bergmann R, Staufenbiel M, Sommer B (2003) Progressive age-related impairment of cognitive behavior in APP23 transgenic mice. Neurobiol Aging 24:365–378.

Koldamova R, Lefterov I (2007) Role of LXR and ABCA1 in the pathogenesis of Alzheimer's disease: implications for a new therapeutic approach. Curr Alzheimer Res 4:171–178.

Koldamova RP, Lefterov IM, Lefterova MI, Lazo JS (2001) Apolipoprotein A-I directly interacts with amyloid precursor protein and inhibits Aβ aggregation and toxicity. Biochemistry 40:3553–3560.

Koldamova R, Staufenbiel M, Lefterov I (2005a) Lack of ABCA1 considerably decreases brain ApoE level and increases amyloid deposition in APP23 Mice. J Biol Chem 280:43224–43235.

Koldamova RP, Lefterov IM, Staufenbiel M, Wolfe D, Huang S, Glorioso JC, Walter M, Roth MG, Lazo JS (2005b) The liver X receptor ligand T0901317 decreases amyloid β production *in vitro* and in a mouse model of Alzheimer's disease. J Biol Chem 280:4079–4088.

LaDu MJ, Falduto MT, Manelli AM, Reardon CA, Getz GS, Frail DE (1994) Isoform-specific binding of apolipoprotein E to β-amyloid. J Biol Chem 269:23403–23406.

LaDu MJ, Pederson TM, Frail DE, Reardon CA, Getz GS, Falduto MT (1995) Purification of apolipoprotein E attenuates isoform-specific binding to β-amyloid. J Biol Chem 270:9039–9042.

Lambert MP, Barlow AK, Chromy BA, Edwards C, Freed R, Liosatos M, Morgan TE, Rozovsky I, Trommer B, Viola KL, Wals P, Zhang C, Finch CE, Krafft GA, Klein WL (1998) Diffusible, nonfibrillar ligands derived from Aβ1–42 are potent central nervous system neurotoxins. Proc Natl Acad Sci USA 95:6448–6453.

Lefterov I, Bookout A, Wang Z, Staufenbiel M, Mangelsdorf D, Koldamova R (2007) Expression profiling in APP23 mouse brain: inhibition of Aβ amyloidosis and inflammation in response to LXR agonist treatment. Mol Neurodegener 2:20.

Lesne S, Koh MT, Kotilinek L, Kayed R, Glabe CG, Yang A, Gallagher M, Ashe KH (2006) A specific amyloid-β protein assembly in the brain impairs memory. Nature 440:352–357.

Maezawa I, Jin LW, Woltjer RL, Maeda N, Martin GM, Montine TJ, Montine KS (2004) Apolipoprotein E isoforms and apolipoprotein AI protect from amyloid precursor protein carboxy terminal fragment-associated cytotoxicity. J Neurochem 91:1312–1321.

Maezawa I, Hong HS, Liu R, Wu CY, Cheng RH, Kung MP, Kung HF, Lam KS, Oddo S, LaFerla FM, Jin LW (2008) Congo red and thioflavin-T analogs detect Aβ oligomers. J Neurochem 104:457–468.

Mauch DH, Nagler K, Schumacher S, Goritz C, Muller EC, Otto A, Pfrieger FW (2001) CNS synaptogenesis promoted by glia-derived cholesterol. Science 294:1354–1357.

McNeish J, Aiello RJ, Guyot D, Turi T, Gabel C, Aldinger C, Hoppe KL, Roach ML, Royer LJ, de Wet J, Broccardo C, Chimini G, Francone OL (2000) High density lipoprotein deficiency and foam cell accumulation in mice with targeted disruption of ATP-binding cassette transporter-1. Proc Natl Acad Sci USA 97:4245–4250.

Miao J, Vitek MP, Xu F, Previti ML, Davis J, Van Nostrand WE (2005) Reducing cerebral microvascular amyloid-beta protein deposition diminishes regional neuroinflammation in vasculotropic mutant amyloid precursor protein transgenic mice. J Neurosci 25:6271–6277.

Necula M, Kayed R, Milton S, Glabe CG (2007) Small molecule inhibitors of aggregation indicate that amyloid β oligomerization and fibrillization pathways are independent and distinct. J Biol Chem 282:10311–10324.

Oram JF, Heinecke JW (2005) ATP-binding cassette transporter A1: a cell cholesterol exporter that protects against cardiovascular disease. Physiol Rev 85:1343–1372.

Pfrieger FW, Barres BA (1997) Synaptic efficacy enhanced by glial cells *in vitro*. Science 277:1684–1687.

Riddell DR, Zhou H, Comery TA, Kouranova E, Lo CF, Warwick HK, Ring RH, Kirksey Y, Aschmies S, Xu J, Kubek K, Hirst WD, Gonzales C, Chen Y, Murphy E, Leonard S, Vasylyev D, Oganesian A, Martone RL, Pangalos MN, Reinhart PH, Jacobsen JS (2007) The LXR agonist TO901317 selectively lowers hippocampal Aβ42 and improves memory in the Tg2576 mouse model of Alzheimer's disease. Mol Cell Neurosci 34:621–628.

Shankar GM, Li S, Mehta TH, Garcia-Munoz A, Shepardson NE, Smith I, Brett FM, Farrell MA, Rowan MJ, Lemere CA, Regan CM, Walsh DM, Sabatini BL, Selkoe DJ (2008) Amyloid-β protein dimers isolated directly from Alzheimer's brains impair synaptic plasticity and memory. Nat Med 14:837–842.

Sturchler-Pierrat C, Abramowski D, Duke M, Wiederhold KH, Mistl C, Rothacher S, Ledermann B, Burki K, Frey P, Paganetti PA, Waridel C, Calhoun ME, Jucker M, Probst A, Staufenbiel M, Sommer B (1997) Two amyloid precursor protein transgenic mouse models with Alzheimer disease-like pathology. Proc Natl Acad Sci USA 94:13287–13292.

Tontonoz P, Mangelsdorf DJ (2003) Liver X receptor signaling pathways in cardiovascular disease. Mol Endocrinol 17:985–993.

Town T, Laouar Y, Pittenger C, Mori T, Szekely CA, Tan J, Duman RS, Flavell RA (2008) Blocking TGF-β-Smad2/3 innate immune signaling mitigates Alzheimer-like pathology. Nat Med 14:681–687.

Van Dam D, D'Hooge R, Staufenbiel M, Van Ginneken C, Van Meir F, De Deyn PP (2003) Age-dependent cognitive decline in the APP23 model precedes amyloid deposition. Eur J Neurosci 17:388–396.

Van Dam D, Vloeberghs E, Abramowski D, Staufenbiel M, De Deyn PP (2005) APP23 mice as a model of Alzheimer's disease: an example of a transgenic approach to modeling a CNS disorder. CNS Spectr 10:207–222.

Wahrle SE, Jiang H, Parsadanian M, Legleiter J, Han X, Fryer JD, Kowalewski T, Holtzman DM (2004) ABCA1 is required for normal central nervous system ApoE levels and for lipidation of astrocyte-secreted apoE. J Biol Chem 279:40987–40993.

Wahrle SE, Jiang H, Parsadanian M, Hartman RE, Bales KR, Paul SM, Holtzman DM (2005) Deletion of Abca1 increases Aβ deposition in the PDAPP transgenic mouse model of Alzheimer disease. J Biol Chem 280:43236–43242.

Wahrle SE, Jiang H, Parsadanian M, Kim J, Li A, Knoten A, Jain S, Hirsch-Reinshagen V, Wellington CL, Bales KR, Paul SM, Holtzman DM (2008) Overexpression of ABCA1 reduces amyloid deposition in the PDAPP mouse model of Alzheimer disease. J Clin Invest 118:671–682.

Zhou J, Fonseca MI, Pisalyaput K, Tenner AJ (2008) Complement C3 and C4 expression in C1q sufficient and deficient mouse models of Alzheimer's disease. J Neurochem 106:2080–2092.

Received 19 February 2009/19 March 2009; accepted 31 March 2009

Published as Immediate Publication 31 March 2009, doi 10.1042/AN20090015